Available online at www.sciencedirect.com
ScienceDirect
Journal of Power Sources 171 (2007) 688–695
JOURNAL OF POWER SOURCES
www.elsevier.com/locate/jpowsour

Adhesion of oxide scales grown on ferritic stainless steels in solid oxide fuel cells temperature and atmosphere conditions

S. Chandra-Ambhorn [a,1], Y. Wouters [a], L. Antoni [b], F. Toscan [c], A. Galerie [a,*]

[a] *SIMAP, INP Grenoble/CNRS/UJF, BP 75, 38402 Saint Martin d'Hères Cedex, France*
[b] *LITEN/CEA Grenoble, 17 rue des Martyrs, 38054 Grenoble Cedex 9, France*
[c] *Ugine & ALZ Research Centre, BP 15, 62330 Isbergues, France*

Received 10 January 2007; received in revised form 14 May 2007; accepted 3 June 2007
Available online 23 June 2007

Abstract

Adhesion of thermal oxide scales grown at 800 °C on ferritic stainless steels F18TNb (AISI 441) and F18MT (AISI 444) proposed as interconnectors in solid oxide fuel cells (SOFCs) was investigated. The effect of oxidising atmosphere – synthetic air or 2% H_2O in H_2 as the representative cathode and anode atmosphere respectively – was considered. Using a room temperature tensile test sitting in the SEM chamber, thermally grown oxide scales were forced to spall and their adhesion energy was derived. Adhesion energy, considered as the elastic energy per unit area stored in oxide was determined at the strain of first spallation or at the strain where the derivative of spallation versus strain was maximum. Adhesion energies were shown to lie in the range 10–100 J cm^{-2}. Adhesion values exhibited decreasing values with increasing oxide thickness, with higher values for oxidation in 2% H_2O/H_2 compared to oxidation in synthetic air. The adhesion energy of scales on F18MT was lower than that on F18TNb due to the presence of Mo-containing intermetallic compounds at the metal/scale interface.

Keywords: Stainless steels; SOFC interconnectors; Oxide scales; Chromia; Adhesion; Water vapour

1. Introduction

Interconnector is a part of solid oxide fuel cells (SOFCs) used to separate the fuel-side anode and the air-side cathode of multiple cells when stacked as a series. It also allows transport of electrons from one cell to another and to the external circuit. For conventional SOFCs working at around 1000 °C, ceramic materials such as doped lanthanum chromite have been proposed as interconnector [1]. However, the attempt is made nowadays to decrease the working temperature of SOFCs to 650–900 °C. At these working temperatures, stainless steels are considered as promising materials to be applied as interconnectors [2,3], primarily due to their gas-tight property and high electrical conductivity. Economic advantages – relatively low price, availability, easy fabrication – compared to ceramic materials are also of importance. Among the various types of stainless steels, ferritic materials have been selected because of their low coefficient of thermal expansion, more compatible than austenitics to the ceramic electrolyte and to the electrode materials. In this work, attention has been paid to two industrial ferritic grades, F18TNb (AISI 441) and F18MT (AISI 444), both containing 18% Cr, recommended for use in high temperature environments. It must be noted that these materials do not contain any reactive element contrary to the specially designed interconnector steels like Crofer 22 APU (Fe–23Cr–Ti–La) and ZMG 232 (Fe–20Cr–Zr–Hf).

Among several needed properties of the oxide scale which naturally grows on the steels in service, good adhesion is crucial to avoid metal/oxide decohesion which could act as a local infinite electrical resistor inhibiting current flow through the cell. Adhesion of oxide scales on metallic alloys is usually assessed by qualitative observation of the metal/oxide interface or by direct measurement of spallation in service. Only few testing methods have been developed to quantitatively determine the

* Corresponding author. Tel.: +33 476 826 535; fax: +33 476 826 677.
E-mail addresses: sca@kmitnb.ac.th (S. Chandra-Ambhorn), Yves.Wouters@ltpcm.inpg.fr (Y. Wouters), Laurent.Antoni@cea.fr (L. Antoni), Francois.Toscan@arcelor.com (F. Toscan), Alain.Galerie@ltpcm.inpg.fr (A. Galerie).
[1] Permanent address: King Monkut's Institute of Technology North Bangkok (KMITNB), 1518 Pibulsongkram Road, Bangsue, Bangkok 10800, Thailand.

0378-7753/$ – see front matter © 2007 Elsevier B.V. All rights reserved.
doi:10.1016/j.jpowsour.2007.06.058

Table 1
Chemical composition of the studied interconnect alloys (wt.%)

Grade	Cr	Ni	C	Mn	Si	Al	Ti	Nb	Mo
F18TNb (AISI 441)	17.83	0.1	0.01	0.24	0.60	0.006	0.13	0.55	0.01
F18MT (AISI 444)	17.60	0.1		0.42	0.42		0.16	0.28	2.04

interfacial fracture toughness of oxide scales, such as the indentation test [4] or the inverted blister test [5,6]. However, the first one is not really precise and the second one needs thin metal specimens and a gluing procedure which does not allow measurements of very adhesive scales. In this work, the so-called *in situ* tensile test, allowing continuous observation of surface spallation during increasing applied strain, was used for assessing adhesion of scales on the steel substrates. Oxide scales on interconnector alloys oxidised in synthetic air and in 2% H_2O/H_2 as the representative cathode and anode atmospheres respectively was investigated, leading to quantitative values of scale adhesion in term of adhesion energy. It has to be reminded that one-direction tensile loading of oxidised specimens gives raise to increased in-plane transverse compression which is considered as the driving force for spallation, not so far from what scales suffer during growth and cooling down.

Adhesion results should confirm whether classical ferritic stainless steels with no *reactive element* could grow oxide scales adhesive enough to be used as SOFC interconnectors.

2. Experimental

2.1. Materials and oxidation procedures

F18TNb (AISI 441) and F18MT (AISI 444) stainless steels were supplied by Ugine & ALZ (Arcelor-Mittal Group) as sheets with thickness of 2.0 and 1.2 mm respectively. Their chemical composition is reported in Table 1. It may be noted that their Cr content is about 18%, with different minor elements: Ti and Nb for AISI 441, Ti, Nb and Mo for AISI 444. All samples were cut to the dimensions 2 mm × 1.5 mm, polished up to SiC 1200 grade, degreased and rinsed. Oxidation kinetics in synthetic air was assessed in a thermobalance at 800–1000 °C for oxidation periods up to 100 h. Comparison between oxidation of both steels in air and in 2% H_2O/H_2 was determined in a horizontal furnace at 800 °C during 100 or 200 h. The mean thickness of the oxide scales was calculated from average mass gain, assuming pure chromia formation.

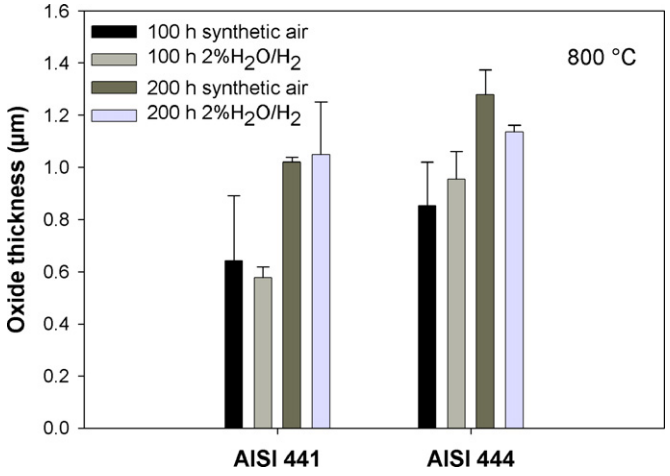

Fig. 2. Oxide thickness on interconnect alloys after 100 and 200 h oxidation runs in synthetic air (cathode atmosphere) or in 2% H_2O/H_2 (anode atmosphere) at 800 °C.

2.2. Determination of oxide scale adhesion energy

Adhesion energy determination by tensile testing was extensively described in previous papers [7–9]. Specimens were

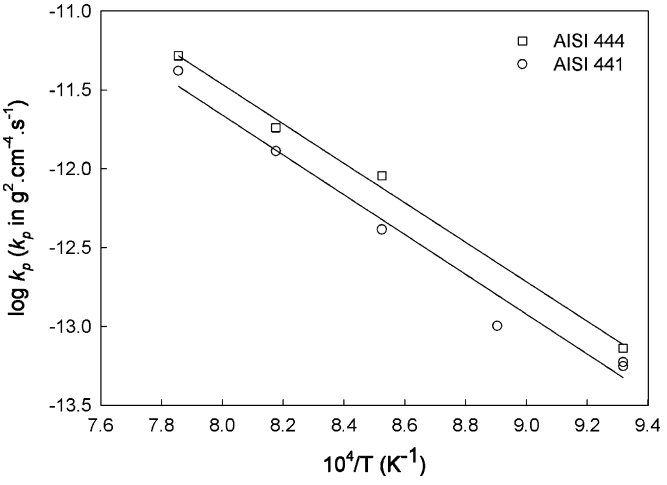

Fig. 1. Evolution with temperature of the parabolic rate constants of oxidation of F18TNb (AISI 441) and F18MT (AISI 444) in synthetic air.

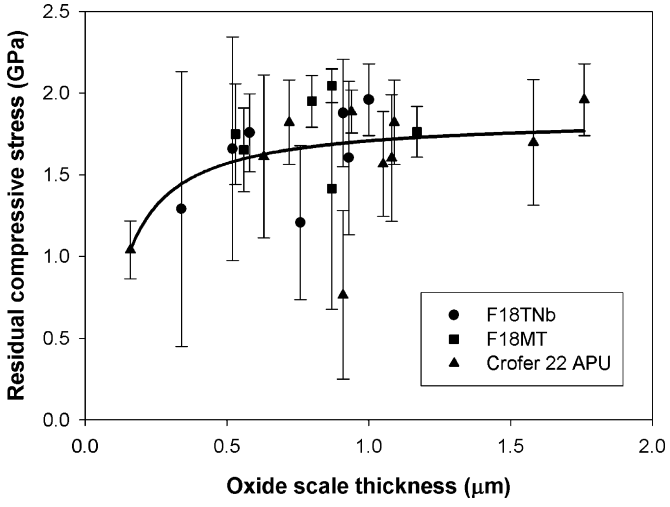

Fig. 3. Compressive residual stress in oxide scales on interconnect alloys in function of oxide thickness. Oxidation in 1 atm. synthetic air at 800 °C.

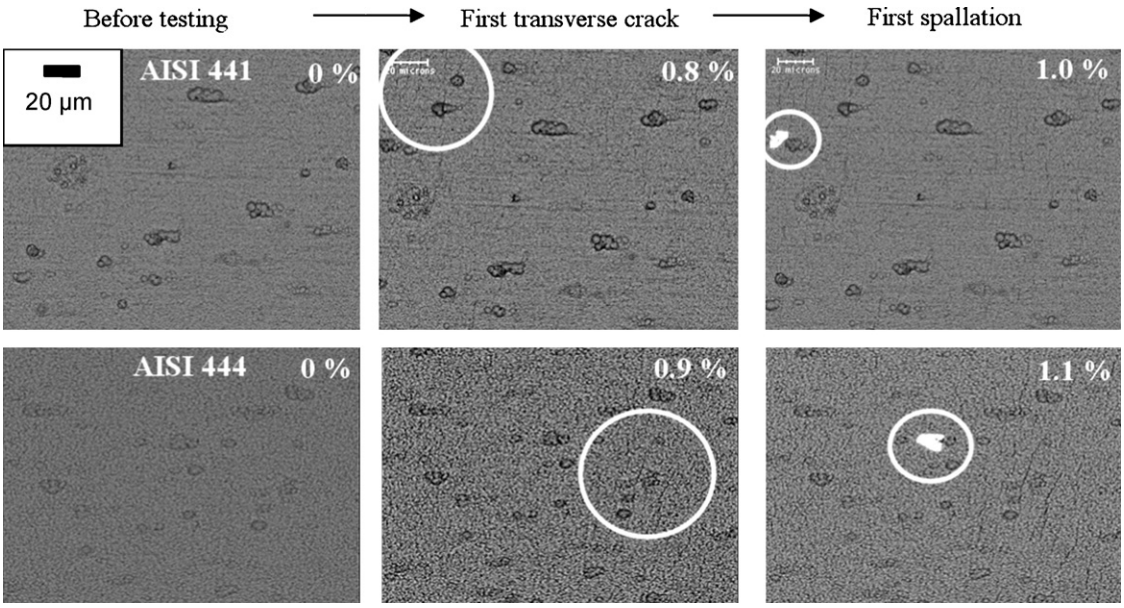

Fig. 4. SEM surface observations of scales on interconnect alloys during the *in situ* tensile test. Scales grown at 800 °C during 200 h in synthetic air. Imposed strain values appear at the top right of the pictures.

prepared by electro-erosion with a special shape fitting to the tensile machine, their main axis parallel to the rolling direction of the sheet. They were polished up to 1200 SiC grit, the final pass of polishing parallel to the main sample axis, rinsed in distilled water and ethanol and dried in air. They were isothermally oxidised in synthetic air or in 2% H_2O/H_2 at 800 °C. Each oxidised specimen was then placed in the tensile machine sitting in the SEM chamber and submitted to constant tensile strain. Sample elongation and tensile load were continuously recorded and transformed into oxide stress and strain. Oxide surface was regularly observed with backscattered electrons and successive pictures were captured at a magnification of 500×. Oxide adhesion energy was identified to interfacial fracture energy and was derived from stress and strain at the first spall, assuming that all mechanical elastic energy stored in the oxide was released by interfacial cracking. All assumptions and calculations used for this determination of adhesion energy were presented in previous papers [7–9]. In the present experiments, parallel through-scale cracking at strain ε_1 occurred far before the first spallation at ε_2. Assumption was therefore made that stress along tensile axis was early released by cracking; observed spallation was assumed to result from transverse compression only.

In order to widen the discussion on adhesion, it was proposed in this work to determine adhesion energy at the strain ε_3 provoking the maximum spallation rate, as a sort of "mean adhesion energy". This new concept is used in Section 3.3.

2.3. Determination of oxide residual stress

In the calculations, room temperature compressive residual stress values in the chromia scales before tensile loading have to be known. These values were determined by Raman

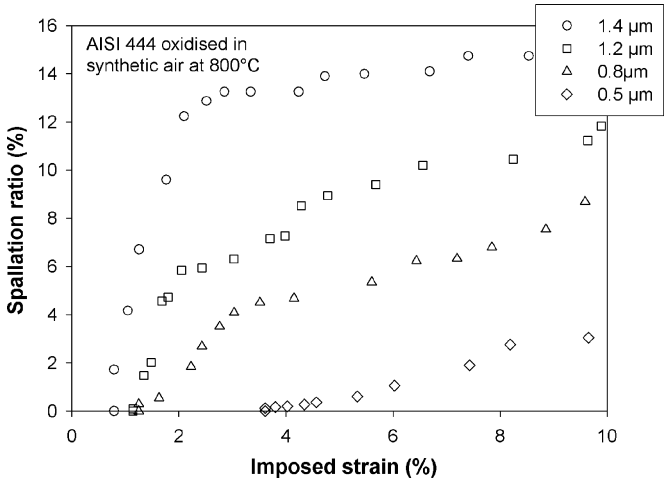

Fig. 5. Fraction of surface area spalled during the tensile test for AISI 444 oxidised in synthetic air at 800 °C.

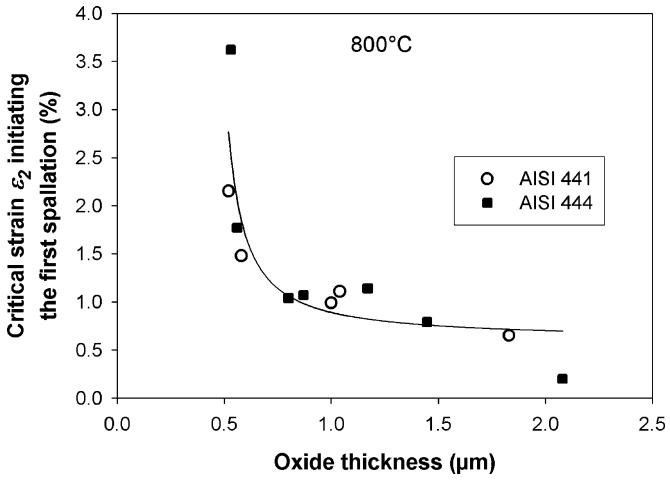

Fig. 6. Strain initiating spallation as a function of oxide thickness. Oxidation in synthetic air at 800 °C.

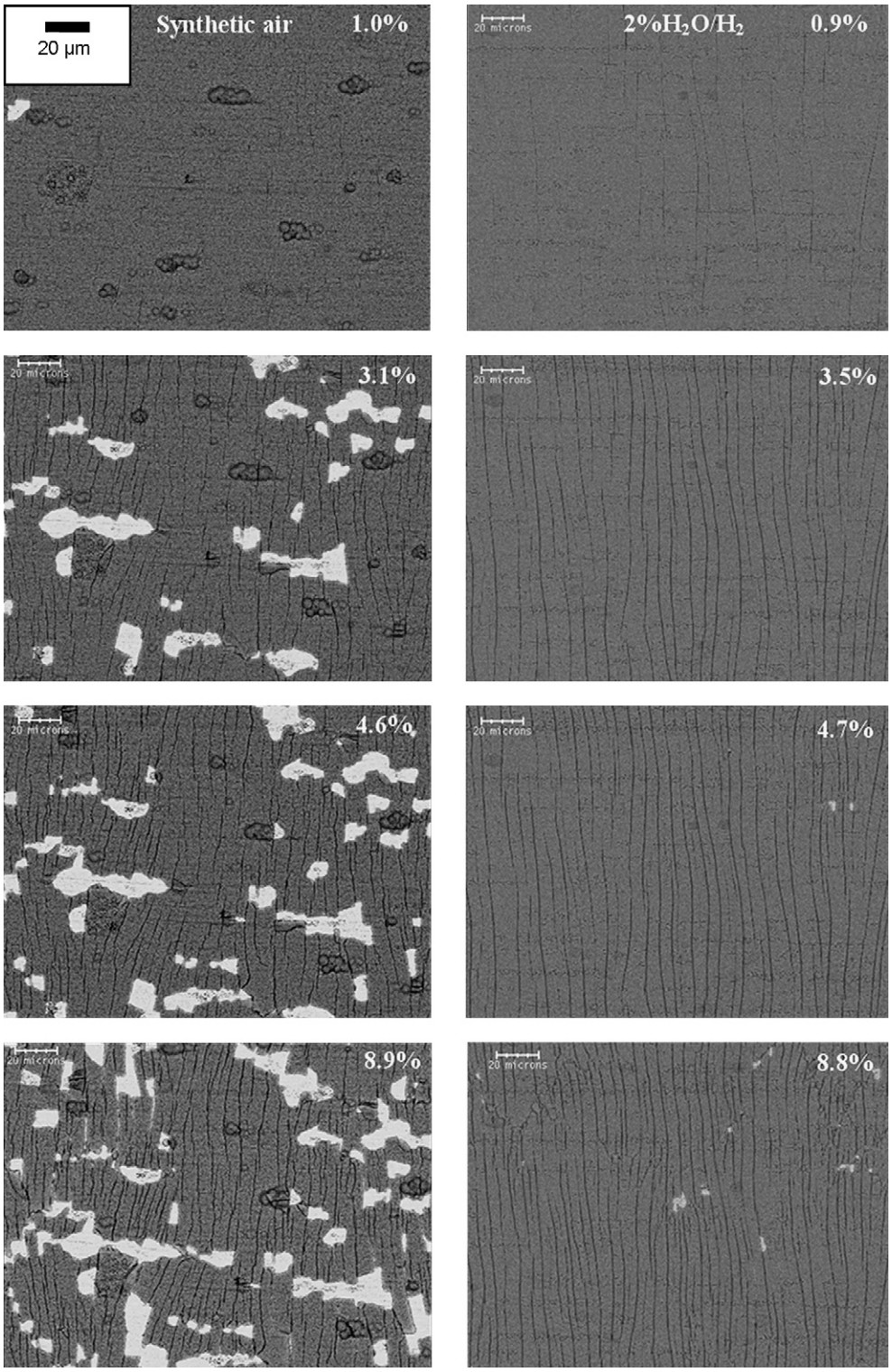

Fig. 7. Spallation of oxide scale on AISI 441 oxidised at 800 °C during 200 h in synthetic air (left) and in 2% H_2O/H_2 (right).

spectroscopy using the green line at 514.53 nm from an argon laser. The most intense Raman peak from chromia was used (554 cm^{-1}) and the Raman shift in function of chromia stress was taken from references [15,16]. For each specimen, the measurement was repeated five times at different sample locations and the given point is the mean value of the five measurements.

3. Results

3.1. Oxidation kinetics

As generally found for stainless steels [10–12], the grown oxide in both atmospheres was mainly chromia Cr_2O_3 forming

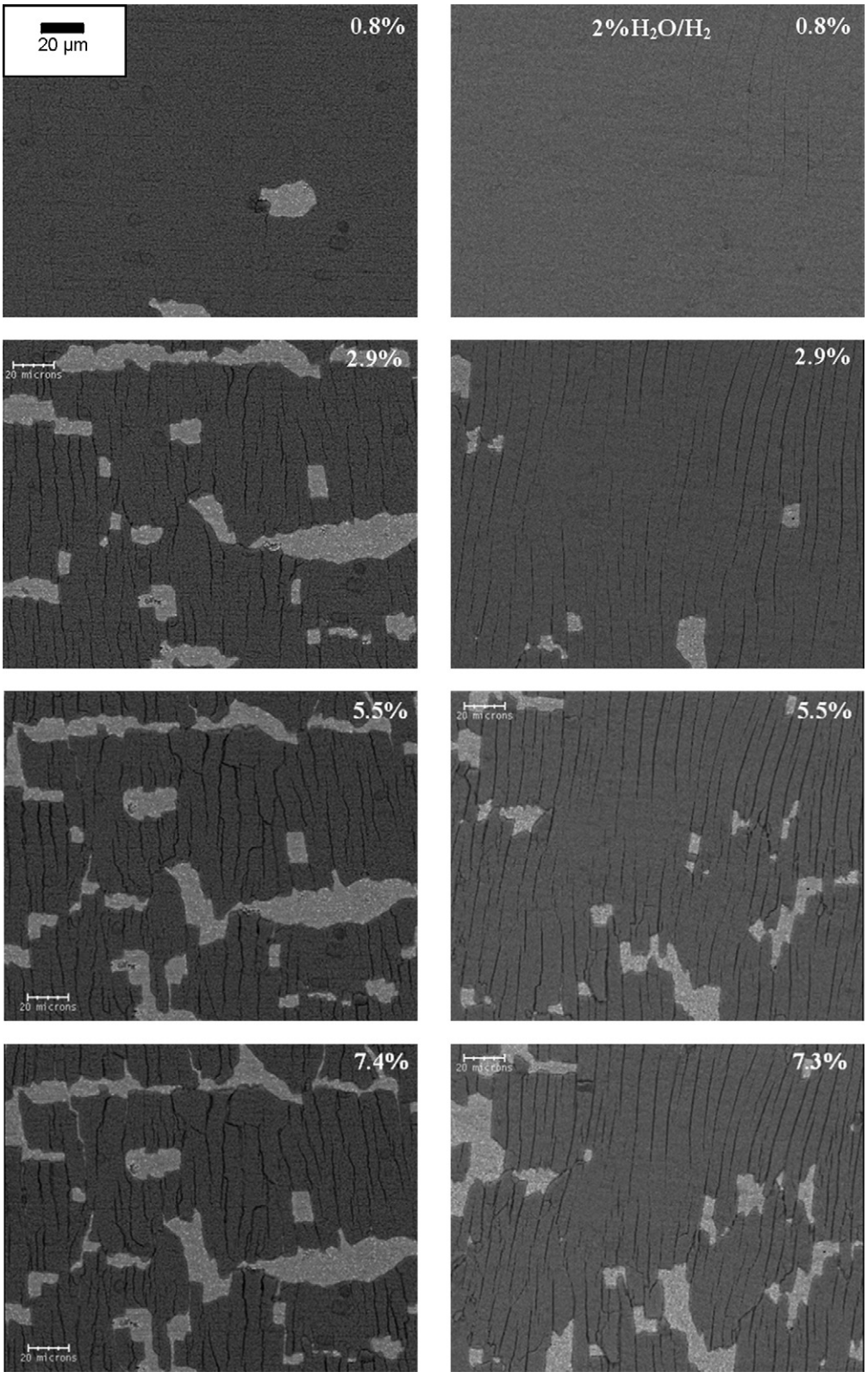

Fig. 8. Spallation of oxide scale on AISI 444 oxidised at 800 °C during 200 h in synthetic air (left) and in 2% H_2O/H_2 (right).

a compact scale, with a top enrichment in manganese in form of $(Mn,Cr)_3O_4$ spinel.

Oxidation kinetics was assessed for AISI 441 and AISI 444 submitted to synthetic air at 800–1000 °C in a thermobalance for oxidation periods up to 100 h. Experiments showed that all oxidations obeyed the parabolic rate law $(\Delta m/A)^2 = k_p t$, with $\Delta m/A$ the weight gain per unit area, t the duration of oxidation and k_p is the parabolic rate constant.

A general observation was that the parabolic rate constants for AISI 444 were slightly higher (1.5×) than those for AISI 441. All parabolic rate constants were plotted in the Arrhenius form in Fig. 1. The apparent activation energy on k_p was derived from the slopes of the curves and was shown to share the same value: $240 \pm 5\ \text{kJ mol}^{-1}$. This observation showed that the mechanisms involved in oxidation were similar, with a rate difference for (at least) one limiting elementary step: chromium diffusion in the steel and/or chromium ion diffusion in the chromia scale.

Comparison between oxidation of both steels in air and in 2% H_2O/H_2 was determined in a horizontal furnace at 800 °C during 100 or 200 h. The mean thickness of the oxide scales was calculated from average mass gain, assuming pure chromia formation and is given in Fig. 2. From this figure, it was confirmed that AISI 441 had the best oxidation resistance in air but also in the H_2O/H_2 anode atmosphere. It also appeared that the oxidation rate of the alloys AISI 441 and AISI 444, was identical in both anode and cathode atmospheres, in agreement with already published results [13,14] showing that the defect structure of chromia was highly changed from p-type chromium vacancy-rich to n-type chromium interstitial-rich when changing air to 2% H_2O/H_2.

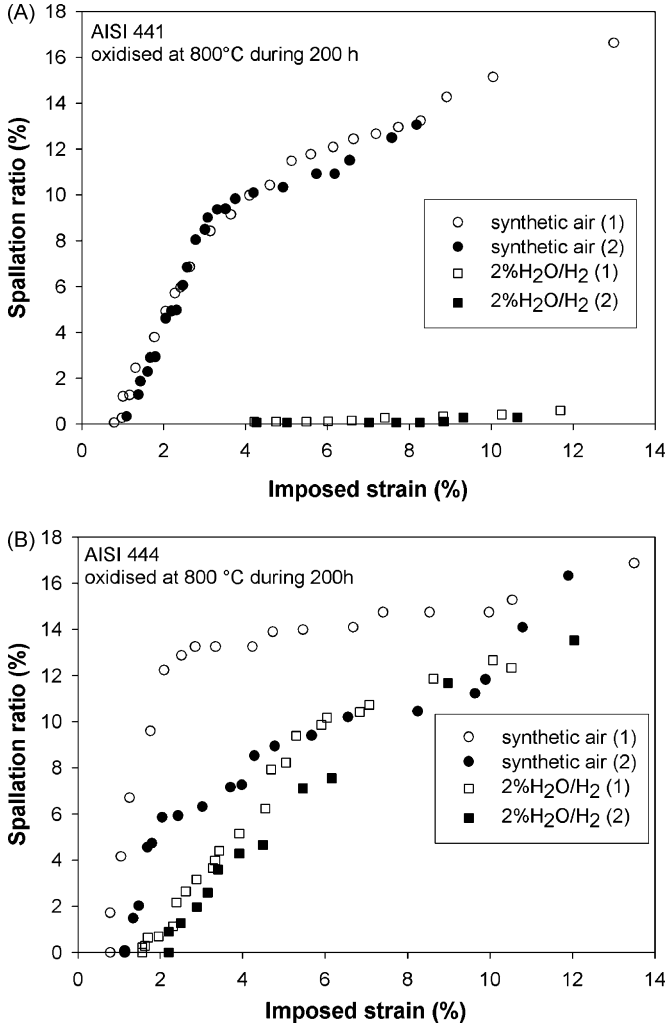

Fig. 9. Spallation ratio during the tensile test of (A) F18TNb (AISI 441) and (B) F18MT (AISI 444) oxidised at 800 °C during 200 h in synthetic air and in 2% H_2O/H_2. (1) and (2) in legend refer to two different samples for each grade.

3.2. Oxide stress values

Fig. 3 presents the values of compressive residual stresses in the formed chromia scales in function of oxide thickness. Results concern both ferritic steels studied in this work and data concerning the ferritic stainless steel Crofer 22 APU (Fe–22.8 Cr–Ti,La), specially designed for SOFC interconnector application, are also shown as a reference. It appeared that, for all steels, the residual stress increased as a function of oxide thickness for very thin scales up to of 0.75 μm and tended to a constant compressive stress of about 1.75 GPa, a value comparable to what was already observed for various ferritic stainless steels [15].

3.3. Qualitative assessment of scale adhesion

3.3.1. Effect of oxide thickness

Fig. 4 depicts the evolution of scale failure during tensile testing for both steels oxidised in synthetic air at 800 °C for 200 h. The first appearing failure was through-scale transverse cracking at a critical strain ε_1 followed, with further straining, by scale spallation beginning at a critical strain ε_2.

The fraction of surface area spalled during tensile testing samples with various oxide thicknesses was recorded and is plotted as an example in Fig. 5 for F18MT (AISI 444). The critical strain (ε_2) initiating the first spallation was extracted and its evolution against scale thickness appears in Fig. 6. It was observed that ε_2 decreased hyperbolically with increasing oxide thickness, with identical trend for scales on both steels.

3.3.2. Effect of oxidising atmosphere

Both studied grades were comparatively oxidised at 800 °C in synthetic air or in 2% H_2O/H_2 during 200 h. Oxide thickness in both atmospheres was similar (1.0 μm for AISI 441 and 1.3 μm for AISI 444). Fig. 7 concerns AISI 441 and depicts the comparative SEM micrographs taken during tensile testing. The same comparison is presented in Fig. 8 for AISI 444. On these

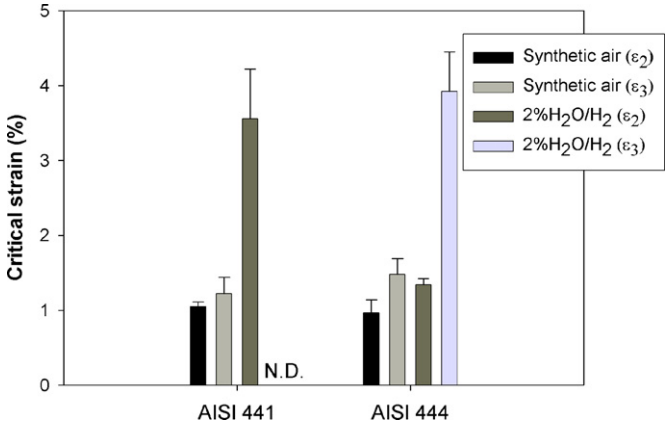

Fig. 10. Critical strain initiating the first spallation of oxide scale on F18TNb (AISI 441) and F18MT (AISI 444) formed in synthetic air and in 2% H_2O/H_2 at 800 °C during 200 h (n.d.: non-determined).

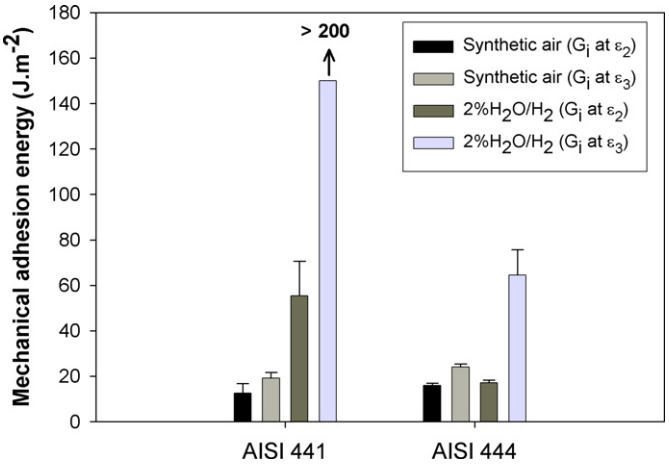

Fig. 11. Adhesion energy of scales on AISI 441 and AISI 444 oxidised in synthetic air and in 2% H_2O/H_2 at 800 °C during 200 h.

photos, it is observed that specimens oxidised in H_2O/H_2 were much less prone to spallation, particularly AISI 441. It was also evident that scales on the three alloys were smoother and less defective in H_2O/H_2. The spallation ratios extracted from these results are shown in Fig. 9 and the critical strains ε_2 appear in Fig. 10. The critical strains (ε_3) provoking the largest spallation ratio with respect to the imposed strain are also added to Fig. 10. The values of ε_3 were obtained at the maximum of the derivative of the spallation ratio versus strain curves of Fig. 9. The qualitative assessment of scale adhesion in terms of strains ε_2 and ε_3 provoking spallation confirmed the good adhesion behaviour of scales grown in the anode atmosphere.

3.4. Quantitative assessment of scale adhesion

Fig. 11 shows adhesion energies determined at ε_2 (first spall) and ε_3 (maximum of the derivative) for scales grown at 800 °C during 200 h in synthetic air and in 2% H_2O/H_2. It was observed that the values lie in the range 10–100 J m^{-2}. From the definition of ε_3, adhesion values at that strain are naturally higher than at ε_2. A first comment is that adhesion energy of scales formed on both alloys in 2% H_2O/H_2 was far larger than that of oxides formed in synthetic air. Comparing now the two grades, it was observed that AISI 441 gave approximately equivalent (slightly less) adhesive scales when grown in air compared to AISI 444. On the contrary, scales grown in 2% H_2O/H_2 were much more adhesive on AISI 441. Also interesting is the use of the "mean adhesion energy" determined at ε_3, which clearly separated situations where the value at the first spall was identical. This was the case for AISI 444 which showed no clear difference between the two atmospheres at ε_2 (Fig. 11), whereas the difference was evident at ε_3.

4. Discussion

A first comment is that the mean adhesion energy in synthetic air was ~20 J m^{-2}, a typical value for high temperature stainless steels. As a matter of discussion, the slightly lower adhesion of scales grown in air on AISI 441 could be the result

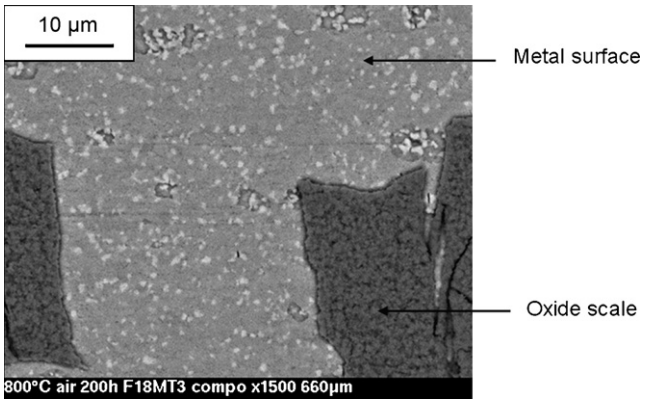

Fig. 12. Mo- and Ti-rich precipitates at the metal/scale interface of AISI 444 oxidised in air at 800 °C during 200 h.

of higher silicon (0.6% instead of 0.42% for AISI 444). This element is known to oxidise to silica at the metal/scale interface, facilitating crack propagation and scale spallation [11]. Another idea is that the large difference observed between the steels in anode atmosphere may be attributed to the presence of high molybdenum in AISI 444. In fact, intermetallic iron–molybdenum precipitates were detected for this grade at the metal/scale interface, as shown in Fig. 12. The stability of these precipitates was assessed by FactSage equilibrium calculations in Fig. 13 which showed that the equilibrium Fe_3Mo_2 intermetallic phase could not be oxidised at the oxygen chemical potential corresponding to the chromium/chromia interface, nor than at the oxygen chemical potential of the 2% H_2O/H_2 atmosphere. As already discussed [6], it seems probable that adhesion of chromia to intermetallic phases containing very low chromium amount is very poor. Another possibility is that these phases hinder intergranular internal oxidation of less noble elements like titanium which are known to improve adhesion.

A great point of interest is the very good adhesion of oxides grown in water vapour compared to what was observed on air for both grades. In our view, this could be the result of an

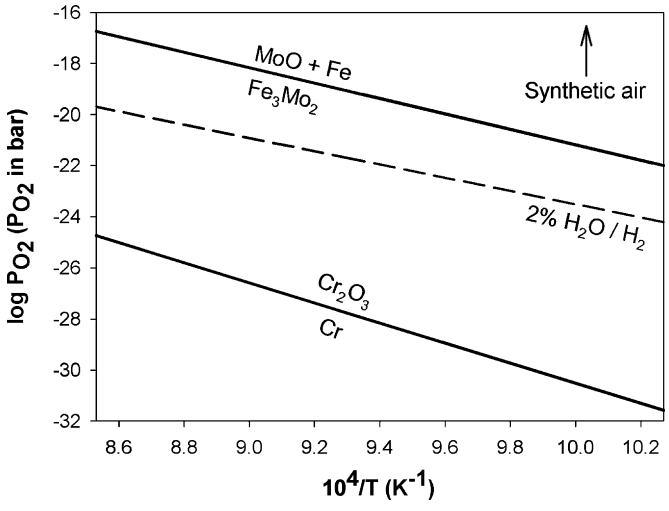

Fig. 13. Thermodynamic stability of Fe_3Mo_2.

increased inward growth of the formed scales which reduced vacancy injection in the alloy, leading to a metal/oxide interface of better quality. Hydroxide species, very mobile in the oxide scale, might be responsible for this modification of the growth direction. The smoother oxide surface in 2% H_2O/H_2 compared to air confirms this inversion of growth direction.

5. Conclusions

The two steels F18TNb (AISI 441) and F18MT (AISI 444), both candidates to be used as interconnectors in SOFCs, were isothermally oxidised in dry synthetic air (cathode atmosphere) and in 2% H_2O/H_2 (anode atmosphere). Oxidation kinetics was determined and tensile loading was used to determine adhesion energy. From the results, the following conclusions could be drawn:

1. F18TNb oxidised more slowly than F18MT.
2. It was confirmed that scales of rather the same thickness were formed on both steels in the cathode and 2% H_2O/H_2 anode atmospheres for the same conditions.
3. Surfaces of scales grown in the H_2O/H_2 anode atmosphere appeared more homogeneous and smoother.
4. Oxides grown in both atmospheres on F18TNb and F18MT could be tested by tensile loading, giving through-scale transverse cracking followed by scale spallation.
5. The adhesion energy at the strain initiating the first spallation (ε_2) was found in the range 10–100 J m^{-2}. Adhesion energy was higher for scales grown in the reducing atmosphere due to the possible participation of hydrogen-containing species diffusing inwards in the oxide during scale growth. Failure of interconnectors by decohesion is therefore not awaited on the anode side. On the cathode side, surface modification of the steels may be envisaged if adhesion increase is necessary.
6. Regarding oxidation kinetics and oxide scale adhesion, F18TNb (AISI 441) seems to be a better choice than F18MT (AISI 444). Indeed, this choice must be discussed in relation with the other important properties needed for interconnectors: high oxide electrical conductivity and low chromium(VI) compound volatilisation.

Acknowledgments

This work was conducted in the frame of the 2000–2005 Franco-Thai program "Eng. 6 Human Resources Development and Joint Research Program in Corrosion Science and Engineering" between INP-Grenoble and KMITNB and was part of the PhD thesis of S. Chandra-Ambhorn who is indebted to the French and Thai governments for a 3-year PhD grant in France. Collaboration between INP-Grenoble, CEA-Grenoble and Ugine & ALZ (Arcelor-Mittal group) allowed efficient development of the project.

References

[1] W.Z. Zhu, S.C. Deevi, Mater. Sci. Eng. A384 (2003) 227–243.
[2] W.J. Quadakkers, J. Pirón-Abellàn, V. Shemet, L. Singheiser, Mater. High Temp. 20 (2) (2003) 115–127.
[3] Y. Zhenkuo, K.S. Weil, D.M. Paxton, J.W. Stevenson, J. Electrochem. Soc. 150 (9) (2003) 1188–1201.
[4] J.L. Beuth, N. Dhanaraj, J. Hammer, S. Laney, F.S. Pettit, G.H. Meier, ASM Materials Solutions Conference and Show, Columbus, OH, October 18–24, 2004.
[5] J. Mougin, M. Dupeux, A. Galerie, L. Antoni, Mater. Sci. Technol. 18 (2002) 1217–1220.
[6] J. Mougin, M. Dupeux, L. Antoni, A. Galerie, Mater. Sci. Eng. A359 (2003) 44–51.
[7] A. Galerie, F. Toscan, E. N'Dah, K. Przybylski, Y. Wouters, M. Dupeux, Mater. Sci. Forum 461–464 (2004) 631–638.
[8] F. Toscan, L. Antoni, Y. Wouters, M. Dupeux, A. Galerie, Mater. Sci. Forum 461–464 (2004) 705–712.
[9] S. Chandra-ambhorn, F. Roussel-Dherbey, F. Toscan, Y. Wouters, A. Galerie, M. Dupeux, Mater. Sci. Technol. 23 (4) (2007) 497–501.
[10] A. Galerie, S. Henry, Y. Wouters, M. Mermoux, J.-P. Petit, L. Antoni, Mater. High Temp. 21 (4) (2005) 9–16.
[11] G. Bamba, Y. Wouters, A. Galerie, F. Charlot, A. Dellali, Acta Mater. 54 (2006) 3917–3922.
[12] S. Chandra-Ambhorn, Ph.D. Thesis, INP Grenoble, 2006 (in English).
[13] T. Brylewski, M. Nanko, T. Maruyama, K. Przybylski, Solid State Ionics 143 (2001) 131–150.
[14] H. Kurokawa, K. Kawamura, T. Maruyama, Solid State Ionics 168 (2004) 12–21.
[15] J. Mougin, T. Le Bihan, G. Lucazeau, J. Phys. Chem. Solids 62 (3) (2001) 553–563.
[16] A. Galerie, J. Mougin, M. Dupeux, N. Rosman, G. Lucazeau, in: P.F. Tortorelli, I.G. Wright, P.H. Hou (Eds.), John Stringer Symposium on High Temperature Corrosion 2001, ASM International, Materials Park, OH, 2003, pp. 138–142.